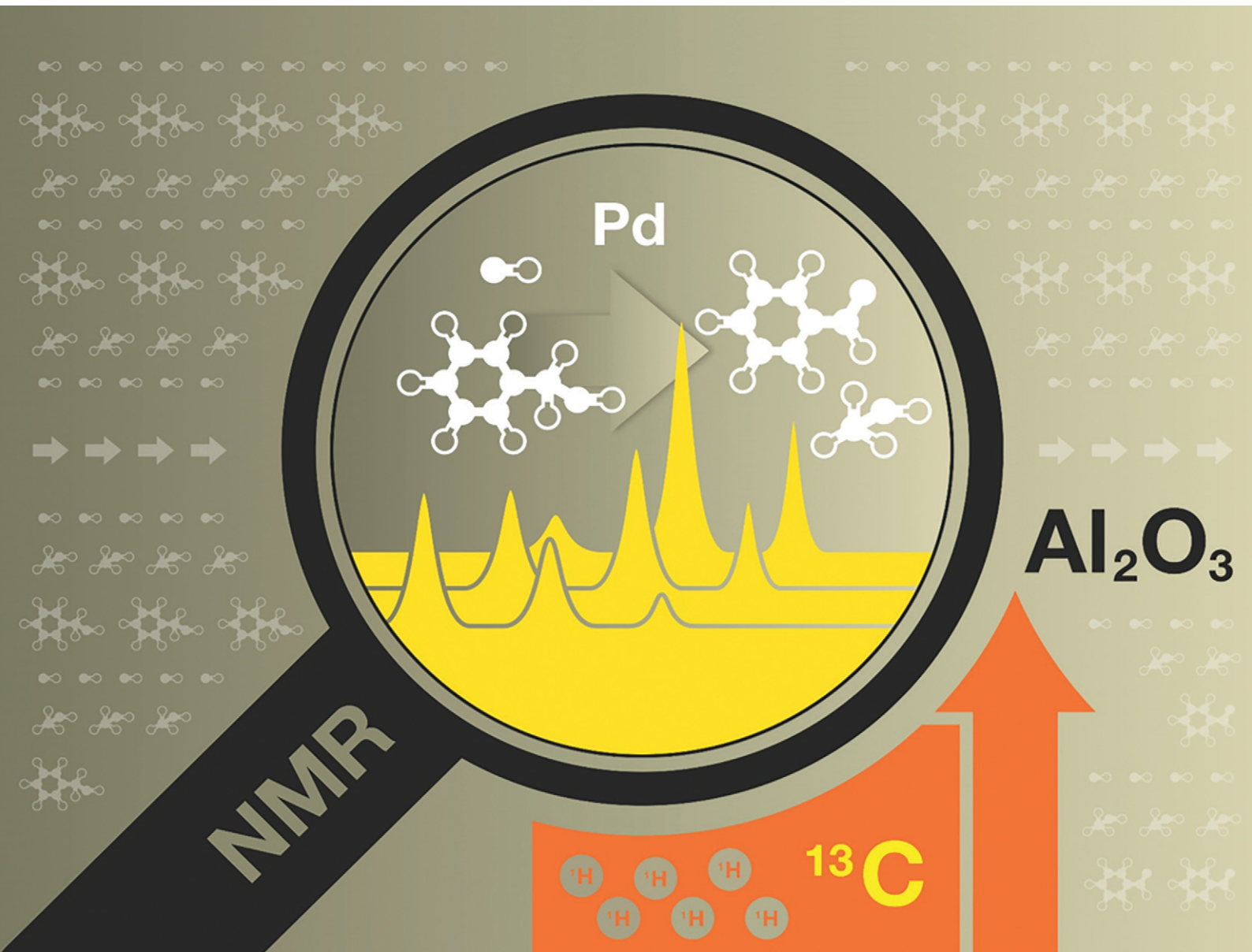


# Reaction Chemistry & Engineering

Linking fundamental chemistry and engineering to create scalable, efficient processes

[rsc.li/reaction-engineering](http://rsc.li/reaction-engineering)





Cite this: *React. Chem. Eng.*, 2020, 5, 1053

Received 23rd December 2019,  
Accepted 28th January 2020

DOI: 10.1039/c9re00489k

rsc.li/reaction-engineering

We report *in situ* high-pressure NMR kinetic studies of catalytic oxidations inside heterogeneous catalysts exploiting distortionless enhancement by polarisation transfer (DEPT)  $^{13}\text{C}$  NMR.  $^1\text{H}$  NMR diffusion and relaxation time measurements are then used to elucidate trends in reaction kinetics in different solvents. The work shows the feasibility of non-invasively monitoring intra-particle kinetics, transport and adsorption in porous catalysts using a comprehensive NMR toolkit.

The application of NMR spectroscopy to study chemical reactions in solid catalysts has grown in recent years. The approach offers several advantages as it allows one to carry out reaction studies non-invasively, exploiting the intrinsic ability of NMR to resolve the structure of chemical species formed during reaction and, unlike conventional approaches based on analysis of bulk fluids surrounding the catalyst particles, allows probing directly chemical kinetics and composition within the catalyst particles. Using such an approach it becomes possible to resolve chemical compositions of species inside the pore space, as for example in heterogeneous catalysis. This has recently been demonstrated when monitoring the evolution of conversion and product distribution during the heterogeneous catalytic ethene oligomerisation reaction at 110 °C and 28 barg over a 1 wt% Ni/SiO<sub>2</sub>–Al<sub>2</sub>O<sub>3</sub> catalyst.<sup>1</sup>

Several other examples of such studies have been reported in the literature. For example, Koptyug *et al.*<sup>2</sup> have used  $^1\text{H}$  NMR to produce spatially resolved spectra within a 2D slice along the axial direction of a fixed bed of 1% Pd/Al<sub>2</sub>O<sub>3</sub>

## *In situ* high-pressure $^{13}\text{C}/^1\text{H}$ NMR reaction studies of benzyl alcohol oxidation over a Pd/Al<sub>2</sub>O<sub>3</sub> catalyst†

Carmine D'Agostino, \*<sup>ab</sup> Mick D. Mantle <sup>a</sup> and Lynn F. Gladden <sup>a</sup>

catalyst pellets. The reaction considered was that of the hydrogenation of  $\alpha$ -methyl styrene to cumene. Although the spectra showed evidence of changes in chemical composition along the length of the bed, no attempt was made to quantify conversion. This was most likely due to problems in deconvolving the broad  $^1\text{H}$  resonances associated with the reactant and product species. In recent work, Leutzsch *et al.*<sup>3</sup> have used  $^2\text{H}$  NMR combined with neutron scattering to monitor the kinetics of the catalytic hydrogenation of benzene in 3 wt% Pt/MCM-41. Catalytic hydrogenation reactions over solid catalysts have also been studied using  $^1\text{H}$  NMR spectroscopy, exploiting parahydrogen-induced polarisation (PHIP) to enhance the NMR signal.<sup>4</sup>

There are cases in which the use of  $^1\text{H}$  NMR becomes prohibitive when studying reactions in solid catalysts as the relatively narrow chemical shift range of the  $^1\text{H}$  nucleus and the line broadening of  $^1\text{H}$  resonances, due to contrast in magnetic susceptibility, give rise to a large number of overlapping resonances, making the resulting NMR spectrum almost featureless and any further analysis difficult if not impossible. In such cases,  $^{13}\text{C}$  NMR spectroscopy is undoubtedly the preferred approach. The principle disadvantage of  $^{13}\text{C}$  NMR is the low signal-to-noise ratio, due to both low natural abundance (~1%) and low sensitivity of the  $^{13}\text{C}$  nucleus relative to the  $^1\text{H}$  nucleus. Polarisation transfer techniques such as the distortionless enhancement by polarisation transfer (DEPT)  $^{13}\text{C}$  NMR spectroscopy technique<sup>5</sup> overcomes some of these disadvantages, enhancing the  $^{13}\text{C}$  signal by up to a factor of four. Moreover, the pulse sequence relies on the  $^1\text{H}$  spin–lattice relaxation time ( $T_1$ ) rather than  $^{13}\text{C}$  spin–lattice relaxation time, which is usually three to five times longer. Therefore, data acquisition can be much faster and this implies a higher signal-to-noise ratio, for a fixed acquisition time. Mantle *et al.*<sup>6</sup> used DEPT  $^{13}\text{C}$  NMR spectroscopy to study hydrogenation and isomerisation of pentenes over commercial Pd/Al<sub>2</sub>O<sub>3</sub> catalyst. When *trans*-2-pentene and hydrogen were both adsorbed onto the support, partial hydrogenation to *n*-pentane was observed in

<sup>a</sup> Department of Chemical Engineering and Biotechnology, University of Cambridge, Philippa Fawcett Dr, Cambridge CB3 0AS, UK. E-mail: cd419@cam.ac.uk, mdm20@cam.ac.uk, lfj1@cam.ac.uk

<sup>b</sup> Department of Chemical Engineering and Analytical Science, The University of Manchester, The Mill, Sackville Street, Manchester, M13 9PL, UK.  
E-mail: carmine.dagostino@manchester.ac.uk

† Electronic supplementary information (ESI) available. See DOI: 10.1039/c9re00489k



addition to the presence of both *cis*-2- and *trans*-2-pentenes. All pentene isomers hydrogenated over the Pd/Al<sub>2</sub>O<sub>3</sub> catalyst to give predominantly *n*-pentane and a small amount of the *trans*-2-pentene isomer. <sup>13</sup>C DEPT-MRI was also used by Sederman *et al.*<sup>7</sup> to spatially map the isomerisation and hydrogenation of 1-octene over Pd/Al<sub>2</sub>O<sub>3</sub> occurring within a trickle-bed reactor.

Whilst hydrogenation reactions over solid catalysts have so far been benefitting from *in situ* NMR spectroscopy, according to our knowledge there has not been any report on catalytic oxidations occurring in porous catalysts. The methodology, if successfully validated, would represent an invaluable tool to study such reactions. Indeed, in recent years there has been growing attention to catalytic oxidations that make use of atmospheric oxygen as the oxidant. This type of reaction is of particular interest as it represents a more sustainable and alternative route to conventional processes using hazardous inorganic oxidizing agents (*e.g.*, H<sub>2</sub>Cr<sub>2</sub>O<sub>7</sub>, KMnO<sub>4</sub>), which tend to produce large amounts of hazardous waste.

In this work, we studied the aerobic catalytic oxidation of benzyl alcohol over a Pd/Al<sub>2</sub>O<sub>3</sub> catalyst (supplied by Johnson Matthey, 0.5% Pd by weight, 2.5 mm trilobes, surface area of approximately 100 m<sup>2</sup> g<sup>-1</sup>) at room temperature (20 °C) using air at high pressure (21 bar) as source of oxygen. The reaction was carried out in a home-built batch reactor, made with NMR-compatible materials, and exploiting *in situ* DEPT-45 <sup>13</sup>C NMR spectroscopy using <sup>13</sup>C natural-abundance species. Oxidation of pure benzyl alcohol as well as benzyl alcohol dissolved in primary aliphatic alcohol solvents (methanol, ethanol and 1-propanol) was chosen as the model system to validate the proposed methodology. The NMR batch reactor was built using polyether ether ketone (PEEK), a thermoplastic polymer with excellent mechanical and chemical resistance properties. The reactor was designed to withstand pressures up to 40 bar and was machined in a cylindrical shape with an external diameter of 20 mm (see Fig. S1 in ESI†). The Pd/Al<sub>2</sub>O<sub>3</sub>

catalyst trilobes were first soaked in the reaction mixture, previously purged with nitrogen, for at least 20 hours to make sure the catalyst pores were saturated. The trilobes were then dried on a pre-soaked filter paper to remove any excess liquid on the external surface and transferred into the NMR batch reactor; the pre-soaking of the filter paper prevented liquid from being drawn out of the pores. The cell was then closed, pressurised to 21 bar with air, placed into the magnet and the NMR acquisition started. DEPT-45 <sup>13</sup>C NMR spectra during reaction were acquired over a period of 15 h. Typical acquisition parameters for the DEPT-45 <sup>13</sup>C NMR experiments were: <sup>13</sup>C and <sup>1</sup>H 90° pulses of 20 µs and 25 µs, respectively; 1024 scans; recycle delay of 4 s; evolution delay time, 1/2J<sub>CH</sub>, equal to 3.4 ms; the value of the echo time,  $\tau$ , was chosen to be 1/2J<sub>CH</sub>, where J<sub>CH</sub> is the spin–spin coupling constant for a <sup>13</sup>C–<sup>1</sup>H group and is approximately 145 Hz. All the <sup>13</sup>C NMR spectra were acquired relative to the <sup>13</sup>C resonance of tetramethylsilane (TMS).

Fig. 1 shows the evolution of the <sup>13</sup>C DEPT-45 spectrum as a function of time. The large peak at approximately 130 ppm arise from the overlapping NMR signals coming from the aromatic rings of both benzyl alcohol (reactant) and benzaldehyde (product), hence such peak cannot be used to monitor unambiguously the reaction. However, the unambiguous and clearly distinguishable signals of the –CH<sub>2</sub>– group of benzyl alcohol, at approximately 60 ppm, and that of the –CHO of the benzaldehyde, at approximately 200 ppm, can be used to monitor both kinetics, conversion and selectivity of the reaction. The formation of benzaldehyde, the main oxidation product, is evident by the rising peak at 200 ppm, whereas the benzyl alcohol consumption can be observed by the decreasing signal at approximately 60 ppm. Spectra of similar quality were observed for benzyl alcohol dissolved in aliphatic alcohols. Again, for all solvents studied, the resonances of the –CH<sub>2</sub>– group of benzyl alcohol and that of the –CHO of the benzaldehyde were clearly

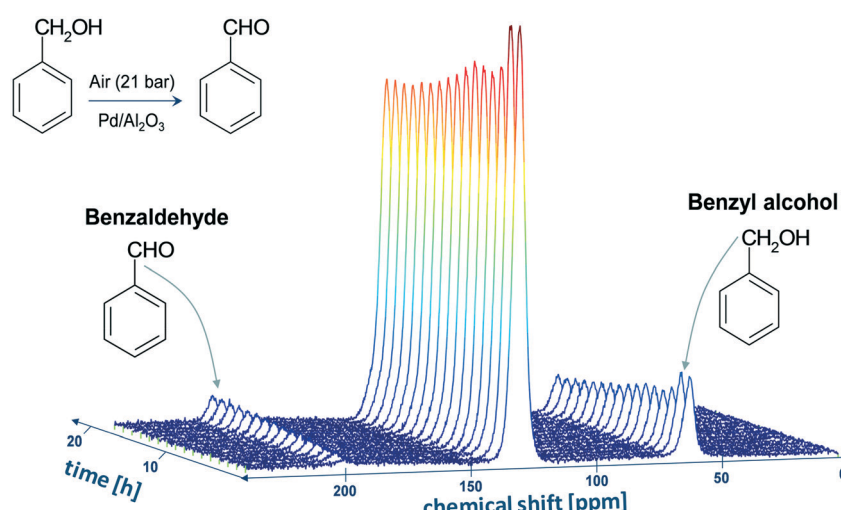


Fig. 1 Evolution of <sup>13</sup>C DEPT-45 NMR spectra during the aerobic catalytic oxidation of benzyl alcohol over Pd/Al<sub>2</sub>O<sub>3</sub> catalyst. The formation of benzaldehyde is clearly evident by the rising NMR signal at 200 ppm, which belongs to the –CHO group of benzaldehyde. Simultaneously, the conversion of the benzyl alcohol is shown by the decrease of the signal at approximately 60 ppm, which belongs to the –CH<sub>2</sub>– group of benzyl alcohol.



distinguishable. No oxidation of the alcohol solvent was observed at the operating conditions chosen for the reaction. It is noted that Pd/Al<sub>2</sub>O<sub>3</sub> catalysts have been reported to be highly selective to convert benzyl alcohol to benzaldehyde with almost 100% selectivity<sup>8</sup> and indeed in our case benzaldehyde was the only oxidation product.

In order to quantify chemical composition using the spectra reported in Fig. 1 several important points need to be considered. The DEPT <sup>13</sup>C NMR signal is influenced by a number of factors that, if not accounted for, will make the acquired signal intensity non-quantitative. These influences are: (a) non-uniform longitudinal relaxation (characterised by  $T_1$ ); (b) non-uniform transverse relaxation (characterised by  $T_2$ ); (c) effects arising from the pulse-sequence itself that leads to differential enhancement of different CH<sub>n</sub> resonances. Non-uniform longitudinal relaxation may be avoided by ensuring a long recycle delay whereas effects arising from differential enhancement of CH<sub>n</sub> resonances can be corrected by considering that the intensity of the peaks of a <sup>13</sup>C DEPT NMR spectrum is described by:<sup>9</sup>

$$I(\text{CH}_n) = n \sin \theta \cos^{n-1} \theta$$

where  $n = 1, 2$  or  $3$  and  $\theta$  is the pulse angle of the final <sup>1</sup>H pulse in the DEPT sequence. Addressing effects arising from non-uniform transverse relaxation ( $T_2$ ) is a more difficult task. Such effects are likely to be present especially when dealing with liquids in porous catalysts, the latter affecting significantly relaxation times of the confined liquids.<sup>10</sup> In principle, the effect of transverse relaxation rate on peak intensity may be predicted by knowing the  $T_2$  value of the peak that needs to be corrected. However, DEPT <sup>13</sup>C NMR involves multiple quantum coherence (mqc) transverse relaxation. Measurements of mqc relaxation rates for pure liquids have been reported by Mlynarik,<sup>11</sup> however, attempts to extend these measurements to heterogeneous systems have not been successful.<sup>12</sup>

In the present work, quantification of DEPT <sup>13</sup>C NMR spectra, in terms of benzaldehyde composition on a solvent-free basis, was carried out using a calibration procedure. Samples of known benzaldehyde composition in benzyl alcohol imbibed in Pd/Al<sub>2</sub>O<sub>3</sub> catalyst pellets, were prepared and DEPT-45 <sup>13</sup>C NMR spectra acquired, keeping the same parameters used to probe reactions. Spectra were acquired at atmospheric pressure and a check to verify that no reaction occurred during the acquisition time of each spectrum was also carried out. No reaction occurred at ambient conditions during the acquisition time. The actual molar composition was compared with the molar composition calculated from NMR spectra by considering the areas of the -CH<sub>2</sub>- peak of benzyl alcohol at 60 ppm and that of the -CHO peak of benzaldehyde at 200 ppm.

Results of the calibration are shown in Fig. 2. It can be clearly seen that the calibration plots are in some cases significantly different from the ideal plot (dotted line). To further investigate the trend in Fig. 2 we carried out  $T_2$  <sup>1</sup>H

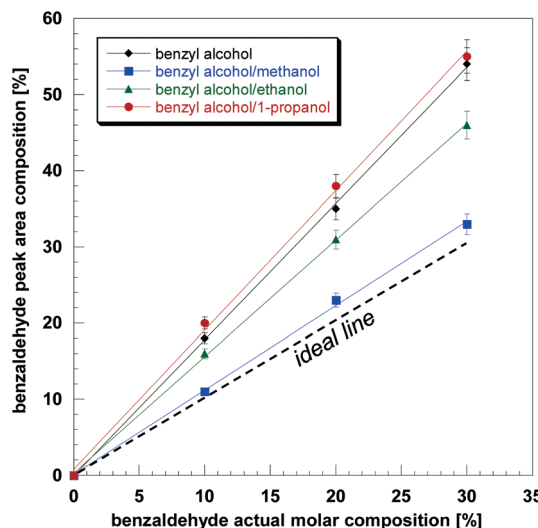


Fig. 2 Calibration plots of <sup>13</sup>C DEPT-45 NMR spectra of benzaldehyde in different benzyl alcohol/solvent mixtures, within Pd/Al<sub>2</sub>O<sub>3</sub> catalyst. Composition of benzaldehyde is solvent-free. Error bars are calculated based on signal-to-noise ratio.

NMR relaxation measurements of benzyl alcohol and benzaldehyde in the absence and presence of solvents with the Pd/Al<sub>2</sub>O<sub>3</sub> catalyst in order to assess any possible effect of non-uniform  $T_2$  relaxation on the DEPT <sup>13</sup>C NMR spectra. Here, it is noted that DEPT <sup>13</sup>C NMR relies on  $T_2$  relaxation of <sup>1</sup>H nuclei and not of <sup>13</sup>C nuclei, which is due to the nature of the pulse sequence (*i.e.*, <sup>1</sup>H-<sup>13</sup>C polarisation transfer). We found that whilst the  $T_2$  of benzaldehyde was approximately the same in all cases (~45 ms), that of benzyl alcohol was significantly shorter (<25 ms) and especially non-uniform across the various solvents. In particular, we observed that the shorter the  $T_2$  of benzyl alcohol the further the calibration curve deviates from the ideal plot. This is because shorter  $T_2$  values of the benzyl alcohol peak lead to a larger drop of its NMR signal, hence making the benzaldehyde composition appearing larger than the actual composition. This implies that there is a significant effect on the spectra due to non-uniform  $T_2$  relaxation; hence quantification through a calibration procedure is needed to correctly quantify intraparticle composition during reaction.

The composition of benzaldehyde within the Pd/Al<sub>2</sub>O<sub>3</sub> catalyst during reaction in different solvents was obtained using the calibration plots of Fig. 2; this was achieved by using the benzaldehyde composition calculated from the NMR peak area measured in a specific solvent (or in solvent-free conditions), hence the vertical axis values of Fig. 2, which were then converted into actual composition, horizontal axis of Fig. 2, using the calibration plot for the solvent (or solvent-free) under investigation. The results are reported in Fig. 3. It can be noted as the benzaldehyde production increases more rapidly in the first 5 h of reaction and then reaches a plateau. Further investigation revealed that such a plateau was due to oxygen depletion. Since air



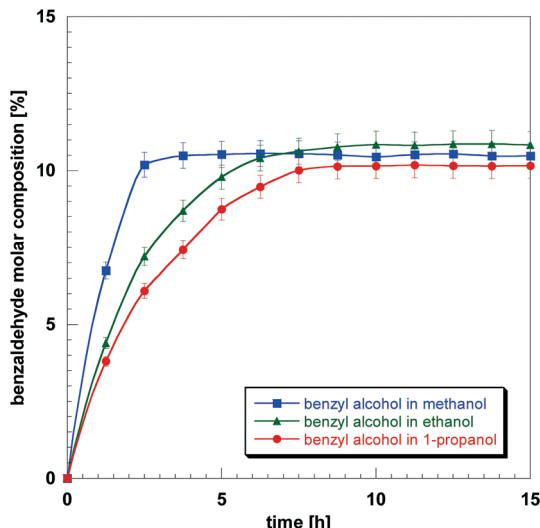
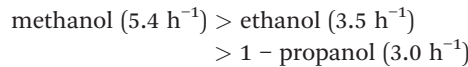


Fig. 3 Evolution of benzaldehyde composition during the course of the oxidation reaction of benzyl alcohol over  $\text{Pd}/\text{Al}_2\text{O}_3$  catalyst. Composition of benzaldehyde is on a solvent-free basis. Solid lines are a guide to the eye. Error bars are calculated based on signal-to-noise ratio.

(approximately 20% oxygen and 80% nitrogen) is used as the oxidant gas, the oxygen consumed is being replaced by air, which eventually leads to accumulation of inert nitrogen and consequent oxygen depletion, stopping the reaction. Indeed, after reaching the plateau, when the reactor was depressurised (purged of used air) and pressurised again with fresh air, the conversion started increasing again, confirming our hypothesis.

From Fig. 3 it is possible to observe differences in reaction rates for different solvents. In particular the initial reaction rate of benzyl alcohol follows the trend:



In order to obtain further insights into such solvent effects, we carried out diffusion measurements of the various reactant/solvent/catalyst systems using  $^1\text{H}$  pulsed-field gradient (PFG) NMR. A typical data set of such measurements is shown in Fig. 4, which shows the  $^1\text{H}$  PFG NMR signal attenuation for an equimolar mixture of benzyl alcohol/1-propanol within the  $\text{Pd}/\text{Al}_2\text{O}_3$  catalyst. The spectrum shows that the peak assignment is unambiguous as it is possible to distinguish the resonances of 1-propanol (0.93, 1.6 and 3.6 ppm) from those of benzyl alcohol (4.6 and 7.4 ppm). The hydroxyl resonances of both alcohols are not present in the spectrum due to  $T_2$ -weighting of the PFG NMR signal. From such spectra it is possible to quantify the diffusion decay of the benzyl alcohol peak in the various solvents and calculate its diffusion coefficient.

In addition to transport properties, we also estimated solvent affinities with the  $\text{Pd}/\text{Al}_2\text{O}_3$  catalyst by calculation of the  $T_1/T_2$  ratio of methanol, ethanol and 1-propanol adsorbed in  $\text{Pd}/\text{Al}_2\text{O}_3$ . Such a ratio has been previously used to assess solvent inhibition in heterogeneous catalysis<sup>13</sup> and gives a good indication of surface adsorption strength.<sup>10</sup> Solvents with a higher  $T_1/T_2$  ratio exhibit stronger interaction with the surface,<sup>14,15</sup> and hence may inhibit a favourable adsorption of the reactant decreasing reaction rate at the surface.

A summary of initial reaction rates, NMR diffusion coefficients and relaxation time measurements is reported in Table 1. The typical relative error for diffusion and  $T_1/T_2$  measurements is approximately 2 and 4%, respectively. It is possible to see a trend in diffusion rate of the reactant in different solvents as well as in  $T_1/T_2$  of the solvent. In particular, solvents with higher reaction rates are associated

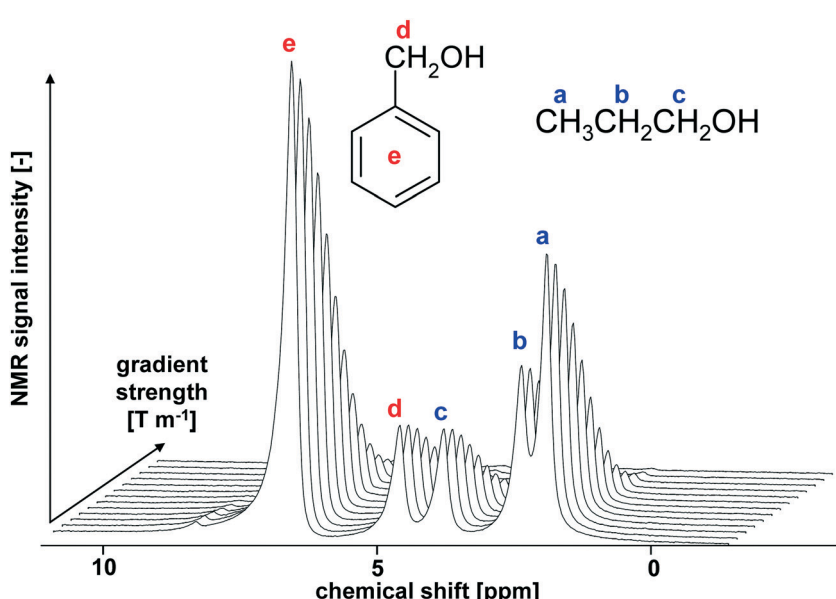


Fig. 4 PFG NMR spectra of an equimolar mixture of benzyl alcohol/1-propanol in  $\text{Pd}/\text{Al}_2\text{O}_3$  catalyst as a function of the gradient strength.



**Table 1** Initial rate, reactant diffusion and  $^1\text{H}$  NMR  $T_1/T_2$  for different solvents in Pd/Al<sub>2</sub>O<sub>3</sub> catalyst

Solvent	Rate [h <sup>-1</sup> ]	$D_{\text{Reactant}}$ [m <sup>2</sup> s <sup>-1</sup> ]	$T_1/T_2$ [-]
Methanol	5.4 ± 0.2	1.85 ± 0.04	20.6 ± 0.8
Ethanol	3.5 ± 0.1	1.69 ± 0.03	29.8 ± 1.2
1-Propanol	3.0 ± 0.1	1.52 ± 0.03	35.0 ± 1.4

to a faster diffusion rate of the reactant and to a lower  $T_1/T_2$  of the solvent, indicating improved transport and a lower degree of solvent inhibition, which leads to favourable adsorption conditions for the reactant over the surface. Such results strongly suggest that both transport and adsorption play an important role in determining catalyst performances. It is interesting to note as a similar trend in  $T_1/T_2$  for primary alcohols in porous oxide catalysts has been reported by Robinson *et al.*<sup>16</sup> in a study involving both NMR and DFT calculations.

In summary, we have reported the first *in situ*  $^1\text{H}$  and  $^{13}\text{C}$  NMR measurements to study aerobic, high-pressure oxidation reactions occurring inside heterogeneous catalysts. The subsequent analysis of the NMR data shows that it is possible to monitor, unambiguously, the evolution of intra-particle composition during the oxidation of benzyl alcohol to benzaldehyde inside Pd/Al<sub>2</sub>O<sub>3</sub> catalyst pellets using air as the oxidant. Moreover, the combination of  $^{13}\text{C}$  NMR measurements, (to extract kinetic information) with measurements of NMR diffusion coefficients and relaxation times gives a more detailed understanding of the physicochemical process of the catalytic system under different working conditions.

## Conflicts of interest

There are no conflicts to declare.

## Acknowledgements

The authors would like to acknowledge Innovate UK for funding this work, Grant No.: TP/7/ZEE/6/I/N0262B. We would also like to thank Dr. Andy York (Johnson Matthey) for providing catalytic materials.

## References

- 1 S. T. Roberts, M. P. Renshaw, M. Lutecki, J. McGregor, A. J. Sederman, M. D. Mantle and L. F. Gladden, Operando magnetic resonance: monitoring the evolution of conversion and product distribution during the heterogeneous catalytic ethene oligomerisation reaction, *Chem. Commun.*, 2013, **49**, 10519–10521.
- 2 I. Koptyug, A. A. Lysova, A. Kulikov, V. A. Kirillov, V. N. Parmon and R. Z. Sagdeev, Functional imaging and NMR spectroscopy of an operating gas-liquid-solid catalytic reactor, *Appl. Catal., A*, 2004, **267**, 143–148.
- 3 M. Leutzsch, M. Falkowska, T.-L. Hughes, A. J. Sederman, L. F. Gladden, M. D. Mantle, T. G. A. Youngs, D. Bowron, H. Manyar and C. Hardacre, An integrated total neutron scattering – NMR approach for the study of heterogeneous catalysis, *Chem. Commun.*, 2018, **54**, 10191–10194.
- 4 K. V. Kovtunov, I. E. Beck, V. I. Bukhitiarov and I. V. Koptyug, Observation of parahydrogen-induced polarization in heterogeneous hydrogenation on supported metal catalysts, *Angew. Chem., Int. Ed.*, 2008, **47**, 1492–1495.
- 5 D. M. Doddrell, D. T. Pegg and M. R. Bendall, Distortionless enhancement of NMR signal by polarization transfer, *J. Magn. Reson.*, 1982, **48**, 323–327.
- 6 M. D. Mantle, P. Steiner and L. F. Gladden, Polarisation enhanced C-13 magnetic resonance studies of the hydrogenation of pentene over Pd/Al<sub>2</sub>O<sub>3</sub> catalysts, *Catal. Today*, 2006, **114**, 412–417.
- 7 A. J. Sederman, M. D. Mantle, C. P. Dunckley, Z. Y. Huang and L. F. Gladden, In situ MRI study of 1-octene isomerisation and hydrogenation within a trickle-bed reactor, *Catal. Lett.*, 2005, **103**, 1–8.
- 8 H. L. Wu, Q. H. Zhang and Y. Wang, Solvent-free aerobic oxidation of alcohols catalyzed by an efficient and recyclable palladium heterogeneous catalyst, *Adv. Synth. Catal.*, 2005, **347**, 1356–1360.
- 9 T. D. W. Claridge, *High resolution NMR techniques in organic chemistry*, Elsevier Ltd, Oxford, UK, 1999.
- 10 C. D'Agostino, J. Mitchell, M. D. Mantle and L. F. Gladden, Interpretation of NMR relaxation as a tool for characterising the adsorption strength of liquids inside porous materials, *Chem. – Eur. J.*, 2014, **20**, 13009–13015.
- 11 V. Mlynarik, Measurement of scalar relaxation of multiple-quantum coherences by spin-echo techniques, *Chem. Phys. Lett.*, 1989, **160**, 25–28.
- 12 C. P. Dunckley, *PhD*, University of Cambridge, 2008.
- 13 C. D'Agostino, M. R. Feaviour, G. L. Brett, J. Mitchell, A. P. E. York, G. J. Hutchings, M. D. Mantle and L. F. Gladden, Solvent inhibition in the liquid-phase catalytic oxidation of 1,4-butanediol: understanding the catalyst behaviour from NMR relaxation time measurements, *Catal. Sci. Technol.*, 2016, **6**, 7896–7901.
- 14 D. Weber, J. Mitchell, J. McGregor and L. F. Gladden, Comparing strengths of surface interactions for reactants and solvents in porous catalysts using two-dimensional NMR relaxation correlations, *J. Phys. Chem. C*, 2009, **113**, 6610–6615.
- 15 A. T. Krzyżak and I. Habina, Low field  $^1\text{H}$  NMR characterization of mesoporous silica MCM-41 and SBA-15 filled with different amount of water, *Microporous Mesoporous Mater.*, 2016, **231**, 230–239.
- 16 N. Robinson, C. Robertson, L. F. Gladden, S. J. Jenkins and C. D'Agostino, Direct Correlation between Adsorption Energetics and Nuclear Spin Relaxation in a Liquid-saturated Catalyst Material, *ChemPhysChem*, 2018, **19**, 2472–2479.

